

# SYNTHESIS OF NI-AL<sub>2</sub>O<sub>3</sub> NANOCOMPOSITE POWDER, ITS CHARACTERIZATION AND DEVELOPMENT BY HVFS TECHNIQUE

Vibhu Sharma<sup>1</sup>, Manpreet Kaur<sup>2</sup> & Sanjiv Bhandari<sup>3</sup>

**Abstract-** In this research work, an attempt has been made to develop a feed stock nanocomposite powder by mechanical alloying method. Nickel (Ni) is selected as a base material. Alumina (Al<sub>2</sub>O<sub>3</sub>) is selected as the reinforcement powder. The reinforced powder is taken in the micro and nano size. The micro Al<sub>2</sub>O<sub>3</sub> powder was milled for 40 hours to obtain the nano sizes particles. The characterisation of the nano powder was done by scanning electron microscopy (SEM) technique. The Ni-Al<sub>2</sub>O<sub>3</sub> powder was prepared in high speed ball milling equipment. The evolution of the different phases, crystalline size and strain has been obtained through X-Ray diffraction test. The composition and morphology of the nanocomposite powder has been studied by scanning electron microscopy and energy dispersive spectroscopy (SEM/EDS) technique. Uniform mixture of the two powders and percentage of all elements has been confirmed by the analysis. Further the powders have been developed by High Velocity Flame Spray (HVFS) technique onto the hydro turbine steels and the as-sprayed coatings have been characterised. The coatings have been successfully developed.

**Keywords:** nano composite powder; ball milling machine; crystalline size; crystalline strain; HVFS spray technique

## 1. INTRODUCTION

The mechanically alloying is a solid-state alloying process in order to combine the advantages of the two-different material. Mechanical milling process involves particles size reduction, mixing or blending and change in the shape of particles. Mechanical alloying is defined as a process of high energy ball milling in which two different powders are experiences a high energy compressive forces action so that they can convert into composite powder under controlled fine microstructure[1]. Different types of equipment's are available for producing the high energy compressive forces such as high speed attritor mills, vibratory mills, shaker mills and high speed planetary ball mills. Planetary ball mill includes a vial of material harder than the milled powder rotates at very high speed. Circular balls of different diameter are used as a milling medium. The RPM of the vial, start-stop time and reversal rotation can be controlled by the programme. Synthesis of intermetallic materials by ball milling has been subject of interest for many researchers in past years[2]–[15]. The mechanical properties of the composite tend to improve with traditionally decreasing the size of the reinforcement particles[16]. This is possibly due to the filling of interstitial spaces by the small sized reinforcement particles. This interstitial space has been created when two different micron size powder are mixed. By filling these voids by nearly nano size reinforcement powder material under the compressive forces in ball milling uniformity of powder can be made figure1. The nano composite of Ni-Al exhibits grain size refinement, and better hardness[17]. The milling time is also a very important parameter for obtaining the uniform distribution of the particle size in intermetallic composite powder. Arif 2015 et al.[18] suggested that homogeneous distribution of Al<sub>2</sub>O<sub>3</sub> can be obtained in Ni-Al<sub>2</sub>O<sub>3</sub> composite powder after 9 hours of ball milling time. High alumina percentage exhibits in Ni-Al composite coating shows lesser volume losses against slurry erosion [19], [20]. An author reported the addition of Al<sub>2</sub>O<sub>3</sub> in tungsten cobalt matrix shows ductile behaviour and found to be useful against the slurry erosion [21].

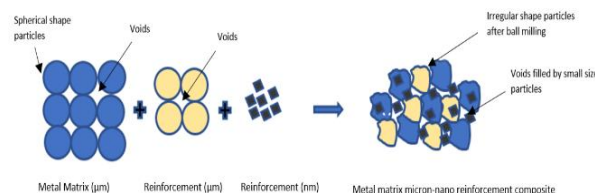


Fig. 1: Possible distribution of matrix ( $\mu\text{m}$ ) and reinforcement ( $\mu\text{m} + \text{nm}$ ) phase in metal matrix composite

<sup>1</sup> Research Scholar, IKG, Punjab Technical University, Jalandhar, Punjab, India

<sup>2</sup> Baba Banda Singh Bhadur College of Engineering and technology, Fathegarh Sahib, Punjab, India

<sup>3</sup> Baba Banda Singh Bhadur College of Engineering and technology, Fathegarh Sahib, Punjab, India

## 2. EXPERIMENTAL

In this investigation, Nickel (Ni), purity of 98.5% particle size 45  $\mu\text{m}$  purchased from Jayesh industry Mumbai, Aluminium Oxide (Al<sub>2</sub>O<sub>3</sub>) purity 99.9% particle size 45 $\pm$ 15  $\mu\text{m}$  were used. For the preparation of the nano size alumina powder particle size 40 micron were charged into the carbide jar of high speed planetary ball milling machine PM100 from RETSCH with balls to powder weight ratio 10:1 to accomplish a fine powder. Initially, 20 grams of powder were charged in the milling jar. The powder was milled for 40 hours and different samples of powder were collected with 3 hours of interval time. Al<sub>2</sub>O<sub>3</sub>-particles were characterized by XRD analysis using an XRD machine (PANalytical X'Pert-Pro, Netherlands), equipped with Cu-K $\alpha$  radiation ( $\lambda=1.5418 \text{ \AA}$ ) under a voltage of 45 kV. The powder samples were scanned at a Goniometer speed of 1 $^\circ$ /minute in the scan range of 10-120 $^\circ$ . In case of ball-milled nano-particles, a small amount of Al<sub>2</sub>O<sub>3</sub> nano-powder were taken after every 15 hr of milling time, 30 hr of milling time and 40 hr of milling time. DLS analysis confirms the particle size of the alumina powder. The morphology of the powder has been seen through scanning emission microscope for different hours of milling time.

Table. 1: Milling parameters used to synthesise Al<sub>2</sub>O<sub>3</sub> nano powder

Mill Details	Milling parameters
Vessel Capacity: 25ml	Milling Atmosphere: Vacuum
Milling Media: Tungsten-Carbide balls	Balls to powder weight ratio: 10:1
Mill Material: Tungsten-Carbide balls	Milling Speed: 450 RPM
PCA: Stearic Acid and Ethanol	Amount of PCA (wt.%): 1.5%-2%
	Milling Time: 40hrs
	Initial Powder: 20 grams

Approximately 20 grams of powder were charged into the tungsten cobalt vial for developing the composite of nickel matrix and alumina oxide as a reinforcement in milling jar. Mechanical milling was done at 250 RPM for 9 hr and 2% of ethanol was added in order to prevent cold welding of the particles. Different phases in each powder is evaluated through CuK $\alpha$ 1 radiation model PANalytical X-pert pro and lattice strain and size of the crystal of each powder has been calculated using Scherrer equation. Hitachi S-800 Field emission scanning electron microscope test evaluated the morphology and compact surface of each elements in the powder. The prepared composite deposited on commonly hydro turbine steel substrate namely CA6NM (0.2% C, 0.9 % Si, 0.72% Mn, 6% Ni, 13% Cr 0.73Mo) by high velocity flame spray technique).

## 3. RESULTS

The results of this section have been divided into three subsections. One and second section describes the synthesis of alumina nano particles and their mechanical allotment with nickel matrix respectively. The later section describes the development of prepared composite powder on hydro turbine substrate by HVFS technique.

### 3.1 Synthesis of Al<sub>2</sub>O<sub>3</sub> Nano Powder

Alumina powder ball milled for the duration of 0 hrs to 40 hrs in high speed ball milling machine. DLS test confirms the optimum particle size 216 nm after 30 hours milling time in fig.2. Fig. 3 shows the decreasing trend of particle size at Different milling time obtained after DLS analysis of samples obtained at different hours. The trend is linear in nature.

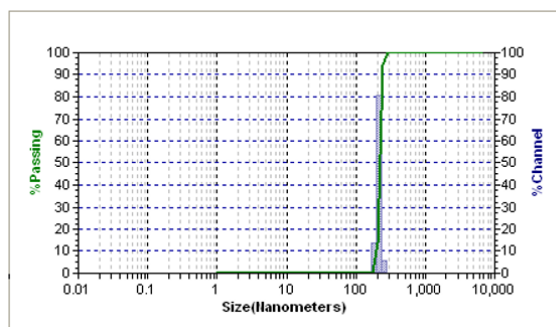


Fig. 2: DLS analysis of Al<sub>2</sub>O<sub>3</sub> Powder after 30 hours milling time

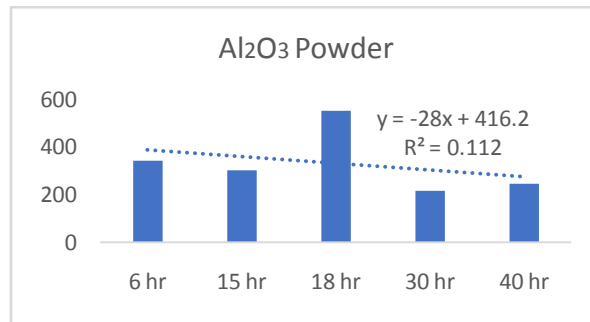


Fig. 3: Linear trend of Al<sub>2</sub>O<sub>3</sub> Powder after different hours milling time

The XRD pattern of alumina powder after 30 hr milling time shows the presence of strong  $\gamma$  phase of alumina at position 27.990°, 38.203°, 48.914°, and weaker  $\alpha$  phase at position 66.974° shown in fig. 4. The average crystalline size and strain present in the particles are 10 nm and 0.778% respectively calculated by Scherrer equation.

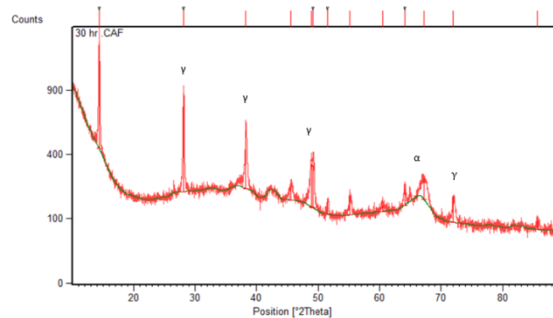


Fig. 4: XRD pattern of Al<sub>2</sub>O<sub>3</sub> Powder after 30 hr milling time

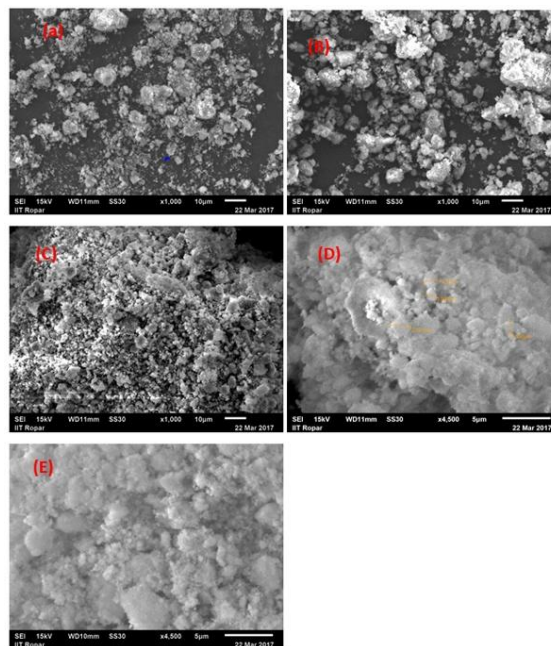


Fig 5: SEM Images of Al<sub>2</sub>O<sub>3</sub> Powder at (A) 12 hr, (B) 15 hr, (C)18 hr, (D) 30 hr and (E) 40 hr milling time

The SEM images of different milling time is shown in fig.5. The morphology of the powder particles appears clusters in shape. The clusters formation is due to the cold welding of powder caused by the compressive forces exerted by the milling balls and rise in temperature during the milling time. The particles look blocky in shape.

### 3.2 Synthesis of Ni-Al<sub>2</sub>O<sub>3</sub> Powder

In this section results are analysed for mechanically alloying the 60%Ni commercial grade and 40%Al<sub>2</sub>O<sub>3</sub> (micron/nano) powder after 9 hours of milling time. Fig.6 shows the SEM morphology of original nickel powder and Alumina powder.

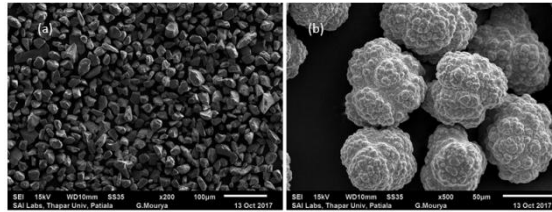


Fig.6: SEM Image of Original (a) Alumina particles (micron size) (b) Nickel particles (micron size)

The synthesis of Ni-Al<sub>2</sub>O<sub>3</sub> powder mechanically mixed in ball mill was confirmed by the X-ray diffraction analysis. As shown in XRD fig.7 almost complete alloying has been achieved after 9 hours of milling time. Ni-Al<sub>2</sub>O<sub>3</sub> is the only crystalline phase that has been detected in the mechanically alloyed powder after 9 hour of milling time. The size of the crystalline and lattice strain is determined from the Scherrer formula and evaluated as 49nm and strain 0.23% respectively. The broadening of high intensity peak may indicate the possible reduction of crystalline size after 9 hour of milling time.

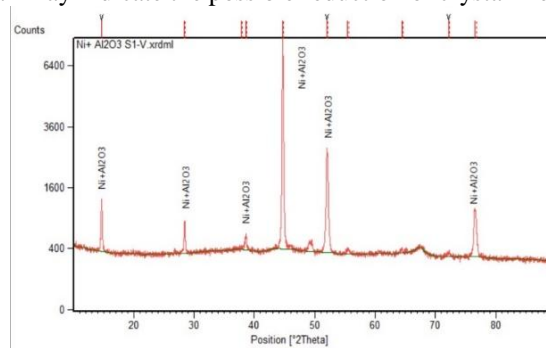


Fig.7: XRD pattern of Ni-Al<sub>2</sub>O<sub>3</sub> after 9 hour of milling time

An angular morphology of the alloyed powder after 9 hours of milling time is seen in scanning electron microscope. As shown in fig.8 the milling of Ni-Al<sub>2</sub>O<sub>3</sub> results the powder agglomeration having a wide range of 10 µm to 0.1 nm. Agglomeration is due to the cold welding of the powder particles during the milling process. The particles appear uniformly distributed and well mixed after the milling process.

The surface EDS of milled powder in fig.9 described the percentage of main elements in the powder. The weight percentage of nickel and aluminium oxide is 1.99% and 33.85 % respectively and rest is of oxygen 64.16 wt.%. This indicate the possible chance of high density nickel layer covered by low density layer of alumina particles.

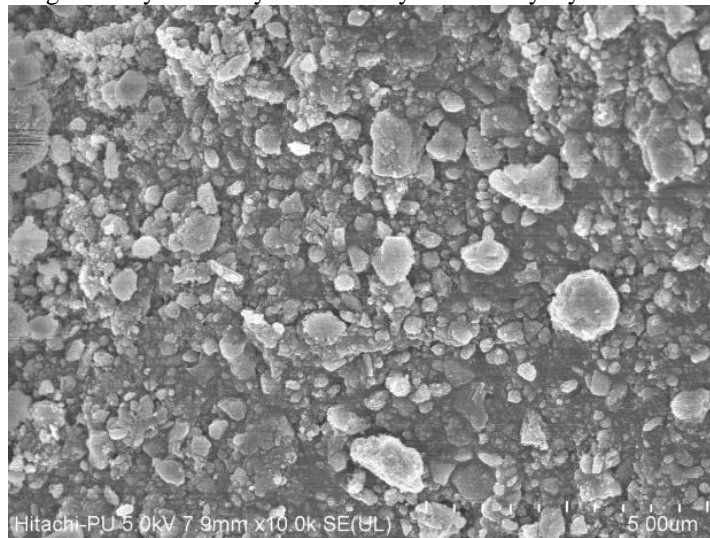


Fig.8: FE-SEM Image of Ni-Al<sub>2</sub>O<sub>3</sub> after 9 hour of milling time

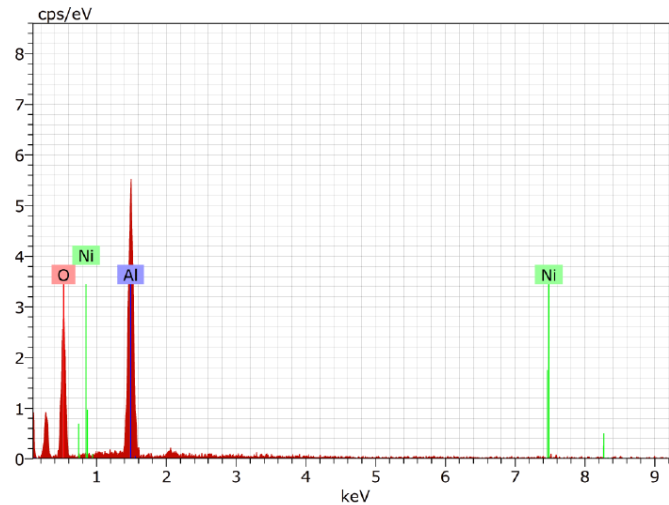


Fig.9: Surface EDS of Ni-Al<sub>2</sub>O<sub>3</sub> after 9 hour of milling time

### 3.3 SEM/EDS Analysis of As-sprayed Coating

SEM micrograph of surface in fig.10 clearly shows the morphology and distribution of the nickel and alumina particles on the substrate. Nickel appears to be splats like shape on the surface however, alumina having a circular shape on the surface. Some of the alumina particles appears un-melted. Moreover, the distribution of alumina particles appears uniform and embed with nickel splats.

The EDS in the fig.11 shows the percentage distribution of the nickel, alumina and oxygen particles on the surface of substrate. Splats are structure slabs of the nickel coating and hence their shape may affect the coatings. The dark phase on the surface is porosity which is less than 4%.

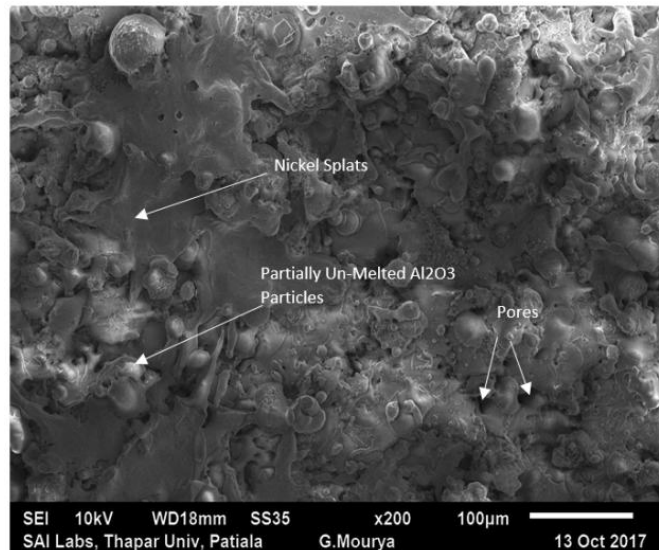


Fig.10: SEM Image of as sprayed Ni-Al<sub>2</sub>O<sub>3</sub> Coating by HVFS tech.

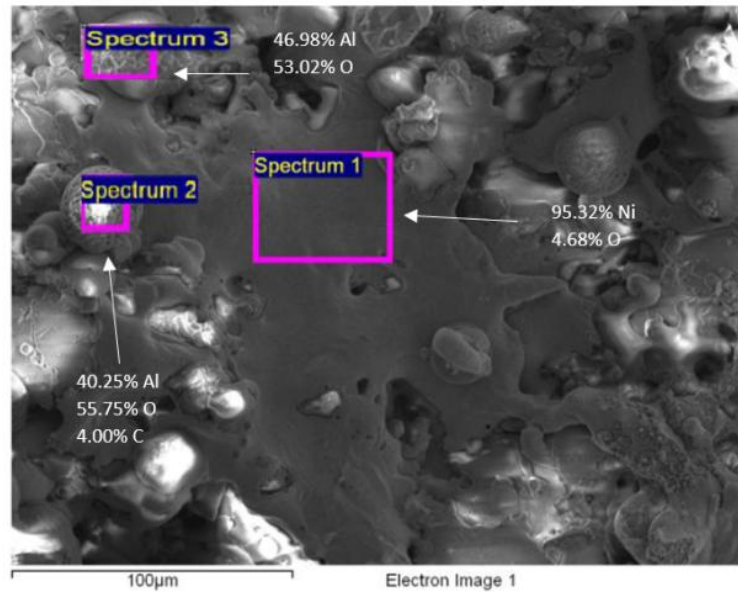


Fig.11: EDS Image of as sprayed Ni-Al<sub>2</sub>O<sub>3</sub> Coating by HVFS tech.

The average surface roughness value of the coating is 8.32  $\mu\text{m}$  because of the high contents of alumina particles [22]. Fig.12 shows the cross-section micrograph image of the coating. The average coating thickness of the coating is 280.8  $\mu\text{m}$ . The bond strength of the coating is evaluated according to ASTM C633-2013 and coating failure is observed at 48.32 MPa.

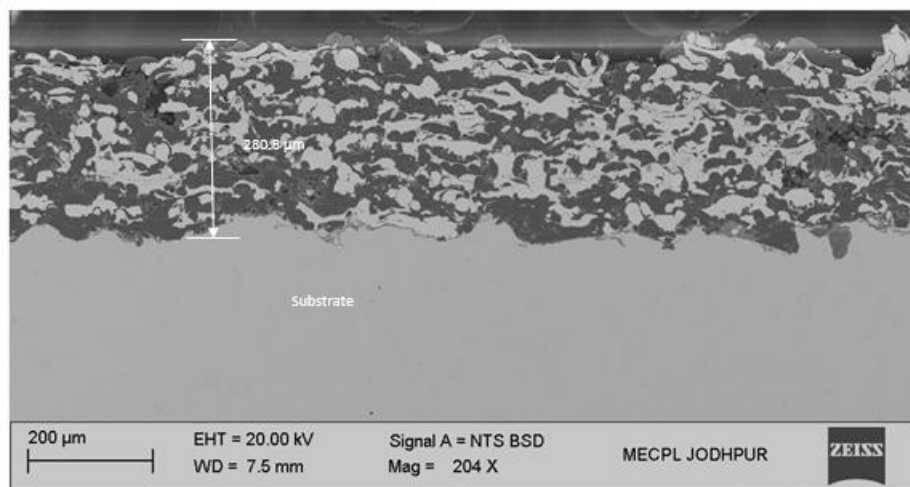


Fig.12: Cross section Image of as sprayed Ni-Al<sub>2</sub>O<sub>3</sub> Coating by HVFS tech.

#### 4. CONCLUSION

1. In DLS analysis nearly nano structured alumina powder is obtained by high speed ball milling machine with average particle size 216 nm after 30 hr of milling time.  $\gamma$  phase of alumina has been observed in X-ray diffraction analysis.
2. Alumina particles appeared in the form of clusters due to cold welding and rise in temperature during the milling process.
3. Ni and alumina were mechanically mixed in the ball milling and coating powder composition was prepared.
4. The crystalline size and strain of the composite has been evaluated using Scherrer equation after X-ray diffraction test and calculated as 49 nm and 0.23% respectively. SEM image of composite powder shows the bulky appearance of the alumina particles attached with nickel powder.
5. The Ni-Al<sub>2</sub>O<sub>3</sub> nano composite coatings were successfully developed on the selected hydro turbine steel by the HVFS spray technique.
6. Microstructure of coatings was composed of evenly distributed alumina particles in a Ni matrix with less porosity.

#### 5. ACKNOWLEDGEMENT

The author wants to thank Dr. Manpreet Kaur and Dr. Sanjeev Bhandari for their intense support for this work. We also thank BBSBEC, Fathegarh Sahib and Punjab University, Chandigarh to providing their research facility.

## 6. REFERENCES

- [1] C. C. Koch, "Materials Synthesis by Mechanical Alloying," *Annu. Rev. Mater. Sci.*, vol. 19, no. 1, pp. 121–143, 1989.
- [2] J. Orea-Lara, H. Balmori-Ramirez, F. J. de Anda-Salazar, and H. Yee-Madeira, "Preparation and characterization of TiN powder by reactive milling in air," *J. Ceram. Process. Res.*, vol. 13, no. 1, pp. 86–88, 2012.
- [3] S. T. Aruna, M. Muniprakash, and V. K. William Grips, "Effect of titania particles preparation on the properties of Ni-TiO<sub>2</sub> electrodeposited composite coatings," *J. Appl. Electrochem.*, vol. 43, no. 8, pp. 805–815, 2013.
- [4] V. V. Dabhade, T. R. Rama Mohan, and P. Ramakrishnan, "Synthesis of nanosized titanium powder by high energy milling," *Appl. Surf. Sci.*, vol. 182, no. 3–4, pp. 390–393, 2001.
- [5] B. Movahedi, "Surface & Coatings Technology Fracture toughness and wear behavior of NiAl-based nanocomposite HVOF coatings," *Surf. Coat. Technol.*, vol. 235, pp. 212–219, 2013.
- [6] J. Kawakita, T. Shinohara, S. Kuroda, M. Suzuki, and S. Sodeoka, "Fabrication of nano-sized oxide composite coatings and photo-electric conversion/electron storage characteristics," *Surf. Coatings Technol.*, vol. 202, no. 16, pp. 4028–4035, 2008.
- [7] A. S. Bolokang and M. J. Phasha, "Formation of titanium nitride produced from nanocrystalline titanium powder under nitrogen atmosphere," *Int. J. Refract. Met. Hard Mater.*, vol. 28, no. 5, pp. 610–615, 2010.
- [8] J. M. Wu, "Nano-sized amorphous alumina particles obtained by ball milling ZnO and Al powder mixture," *Mater. Lett.*, vol. 48, no. 6, pp. 324–330, 2001.
- [9] B. C. Yadav, T. Shukla, S. Singh, and T. P. Yadav, "Titania Prepared by Ball Milling : Its Characterization and Application as Liquefied Petroleum Gas Sensor," pp. 1–19.
- [10] T. T. N. Nguyen and J. L. He, "Preparation of titanium monoxide nanopowder by low-energy wet ball-milling," *Adv. Powder Technol.*, vol. 27, no. 4, pp. 1868–1873, 2016.
- [11] A. S. Bolokang, D. E. Motaung, C. J. Arendse, and T. F. G. Muller, "Production of titanium-tin alloy powder by ball milling: Formation of titanium-tin oxynitride composite powder produced by annealing in air," *J. Alloys Compd.*, vol. 622, pp. 824–830, 2015.
- [12] P. Matteazzi and G. Le Caër, "Synthesis of Nanocrystalline Alumina–Metal Composites by Room-Temperature Ball-Milling of Metal Oxides and Aluminum," *J. Am. Ceram. Soc.*, vol. 75, no. 10, pp. 2749–2755, 1992.
- [13] E. Furlani, E. Aneggi, C. de Leitenburg, and S. Maschio, "High energy ball milling of titania and titania-ceria powder mixtures," *Powder Technol.*, vol. 254, pp. 591–596, 2014.
- [14] D. A. Small, G. R. MacKay, and R. A. Dunlap, "Hydriding reactions in ball-milled titanium," *J. Alloys Compd.*, vol. 284, no. 1–2, pp. 312–315, 1999.
- [15] M. J. Phasha, A. S. Bolokang, and P. E. Ngoepe, "Solid-state transformation in nanocrystalline Ti induced by ball milling," *Mater. Lett.*, vol. 64, no. 10, pp. 1215–1218, 2010.
- [16] C. Suryanarayana, "Recent developments in mechanical alloying," *Rev. Adv. Mater. Sci.*, vol. 18, pp. 203–211, 2008.
- [17] T. Chen, J. M. Hampikian, and N. N. Thadhani, "Synthesis and characterization of mechanically alloyed and shock-consolidated nanocrystalline NiAl intermetallic," *Acta Mater.*, vol. 47, no. 8, pp. 2567–2579, 1999.
- [18] T. M. Arif and N. Saheb, "Characterization of Ball Milled Ni–Al<sub>2</sub>O<sub>3</sub> Nanocomposite Powders," *Powder Metallurgy and Metal Ceramics*, vol. 53, no. 9–10, pp. 541–548, 2015.
- [19] H. S. Grewal, A. Agrawal, and H. Singh, "Tribology International Slurry erosion performance of Ni – Al<sub>2</sub>O<sub>3</sub> based composite coatings," *Tribology Int.*, vol. 66, pp. 296–306, 2013.
- [20] H. S. Grewal, H. S. Arora, A. Agrawal, H. Singh, and S. Mukherjee, "Slurry erosion of thermal spray coatings: Effect of sand concentration," *Procedia Eng.*, vol. 68, pp. 484–490, 2013.
- [21] D. Kumar Goyal, H. Singh, H. Kumar, and V. Sahni, "Slurry erosion behaviour of HVOF sprayed WC-10Co-4Cr and Al<sub>2</sub>O<sub>3</sub>+13TiO<sub>2</sub> coatings on a turbine steel," *Wear*, vol. 289, pp. 46–57, 2012.
- [22] H. S. Grewal, H. Singh, and A. Agrawal, "Microstructural and mechanical characterization of thermal sprayed nickel-alumina composite coatings," *Surf. Coatings Technol.*, vol. 216, pp. 78–92, 2013.